Journal of Applied Mechanics and Technical Physics, Vol. 35, No. 1, 1994

MODELING OF A MONOSILANE RF-DISCHARGE PLASMA

V. A. Shveigert, M. I. Zhilyaev, and I. V. Shveigert

UDC 537.525

A monosilane rf-discharge plasma is investigated by numerical methods. The results of Monte Carlo calculations of the electron kinetics are compared with the results of calculations in the hydrodynamic approximation. It is shown that the hydrodynamic model works well over the entire range of parameters of a plasma-chemical reactor for the deposition of amorphous silicon films. Certain plasma parameters of importance from the standpoint of cooling, such as the dissociation frequency of monosilane and the energy and flux of ions onto the electrodes, are investigated as functions of the discharge power density and the pressure in the reactor in the hydrodynamic approximation.

1. INTRODUCTION

The monosilane (SiH_4) glow-discharge plasma created in a low-pressure plasma reactor during the deposition of thin films of hydrogenated amorphous silicon (α-Si:H) has stimulated considerable interest by virtue of the widespread application of such films as a technological material in microelectronics. Planar plasma-chemical reactors with two parallel electrodes (diode geometry [1]) are most often used to set up the plasma-enhanced chemical vapor deposition (PECVD) of α-Si:H thin films. A mixture of gases is usually delivered through a hole in the upper electrode, and the plate is placed on the lower (grounded) electrode. The following parameters are typical of existing equipment: frequency of the applied voltage f = 13.6 MHz; gas pressure p = 13.3-133.3 Pa; interelectrode spacing D = 1-5 cm; electrode radius R = 5-15 cm; gas flow Q = 10-500 cm^3/min at atmospheric pressure; power density of the discharge W = 0.01-1 W/cm^2.

The optimization of the deposition conditions so as to obtain films having prescribed attributes is a fundamental objective of the numerous experimental studies reported to date and also of diverse model investigations in this direction [1]. For the given reactor configuration, optimization means to select deposition parameters (discharge power density, chamber pressure, substrate temperature, and gas flow through the reactor) that will ensure the deposition of a film of the required quality at an acceptable rate and with uniform growth.

The sum total of the multifarious physicochemical conversions involved in the plasma-chemical reactor can be broken down into three stages: 1) the generation of radicals and ions in the discharge as a result of inelastic interactions of electrons with molecules and atoms of the primary mixture; 2) homogeneous reactions between the formed radicals and ions and molecules of the primary mixture against the background of convection–diffusion transfer (volume chemical kinetics); 3) the kinetics of active particles adsorbed on the surface of the growing film (surface chemical kinetics). The rf-discharge model used to describe the first conversion stage must afford reliable predictions of such important characteristics of the deposition process as the silane dissociation frequency and the energy and flux of ions onto the surface of the growing film.

The most complete model of the plasma-chemical deposition of amorphous silicon from SiH_4 has been presented by Kushner [4-7], who has developed reasonably well-justified model elements describing the volume and surface chemical kinetics, but simulates the rf discharge by a Monte Carlo technique using a model distribution of the electric field, i.e., obtains a solution to a nonself-consistent problem.

The feasibility and sufficiency of the hydrodynamic approximation for describing the rf discharge in the above-indicated range of parameters has been discussed at length (in particular, for electronegative gases of the SF_6 and Cl_2 type used in etching) have been discussed in the literature [3, 11, 12]. Not all the conditions that formally impose limits on the applicability of the

Novosibirsk. Translated from Prikladnaya Mekhanika i Tekhnicheskaya Fizika, No. 1, pp. 13-21, January-February, 1994. Original article submitted March 3, 1993.

0021-8944/94/3501-0013$12.50 © 1994 Plenum Publishing Corporation

hydrodynamic approximation are necessarily in effect at low pressures (p $\approx$ 13.3 Pa). For example, the mean free path of electrons in elastic collisions, $l_e \approx 0.1$ cm, is small in comparison with the discharge gap D (which is usually a few centimeters) ($l_e \ll$ D), but the same is no longer true in relation to the thickness of the electrode sheaths $D_k \approx 0.5$-1 cm. There is some doubt here as to whether the role of γ-electrons emitted from the electrode surfaces is adequate described in the hydrodynamic model. Strictly speaking, the transition to the γ-regime requires a sufficient voltage drop across the layer, the precise value of this voltage depending on the power input. High-quality α-Si:H films are known to build up at moderate power inputs (W $\leq$ 0.1 W/cm^2), but calculations, for example, at W = 0.1 W/cm^2, p = 13.3 Pa, and D = 4 cm have shown that the voltage drop across the layer (of thickness $D_k \approx 1$ cm) is fairly high ($\approx$200 V). To circumvent this shortcoming in relation to γ-electrons, two groups of electrons are considered in the hydrodynamic model proposed below.

We have performed Monte Carlo calculations of the electron kinetics of an rf discharge, specifically for comparison purposes, with a view toward resolving all other conflicting issues concerning the applicability of the hydrodynamic approximation in application to a SiH_4 plasma in the indicated range of parameters.

2. THE MODEL

The one-dimensional rf-discharge model embodies a hydrodynamic description of electrons and ions. The number-density and average-energy transport equations are solved for electrons, and the hydrodynamic equations are solved for positive and negative ions:

$$\frac{\partial N_e}{\partial t} - \frac{\partial\,(\mu_e E N_e + \partial\,(D_e N_e)/\partial x)}{\partial x} = (\nu_i - \nu_a)\,N_e + \nu_d N_n - \nu_b N_e N_p; \tag{2.1}$$

$$\frac{\partial N_e U_e}{\partial t} - \frac{\partial\,(\mu_u E N_e U_e + \partial\,(D_u N_e U_e)/\partial x)}{\partial x} = eE\left(\mu_e E N_e + \frac{\partial D_e N_e}{\partial x}\right) - \nu_u N_e U_e; \tag{2.2}$$

$$\frac{\partial N_p}{\partial t} + \frac{\partial N_p V_p}{\partial x} = \nu_i N N_e - \nu_b N_e N_p - \beta N_p N_n; \tag{2.3}$$

$$\frac{\partial N_n}{\partial t} + \frac{\partial N_n V_n}{\partial x} = \nu_a N N_e - \nu_d N_n - \beta N_p N_n; \tag{2.4}$$

$$\frac{\partial V_p}{\partial t} + \frac{\partial V_p^2/2}{\partial x} = \frac{eE}{M_p} - W_p N V_p; \tag{2.5}$$

$$\frac{\partial V_n}{\partial t} + \frac{\partial V_n^2/2}{\partial x} = \frac{-eE}{M_n} - W_n N V_n. \tag{2.6}$$

The potential distribution Φ is described by the Poisson equation

$$\frac{d^2\Phi}{dx^2} = 4\pi e\,(N_e + N_n - N_p), \quad E = -\frac{d\Phi}{dx}.$$

Here N_e, N_n, and N_p are the densities of electrons, negative ions, and positive ions; ν_i, ν_a, ν_d, and ν_u are the frequencies of ionization, adhesion, dissociation, and inelastic scattering of electrons; μ_e and D_e are the electron mobility and diffusion coefficients; ν_b and β are the electron–ion and ion–ion recombination coefficients, μ_u and D_u are the mobility and diffusion coefficients at the average electron energy U_e; and M_p, M_n, W_p, and W_n are the masses and scattering frequencies of positive and negative ions, respectively.

To determine the transport coefficients involved in Eqs. (2.1) and (2.2), we use the energy distribution function $f_0(\varepsilon)$ of electrons in a uniform electric field, calculating it from the kinetic equation in the binomial approximation:

$$-\frac{\partial}{\partial\varepsilon}\left(\frac{2e^2E^2\varepsilon\partial f_0}{3mN\sigma_t\partial\varepsilon}\right) = \mathrm{St}\,\{f_0\}.$$

Here σ_t is the transport scattering cross section, m is the electron mass, and the collision term St$\{f_0\}$ includes only inelastic collisions. The error of the binomial approximation in nonuniform static electric fields is discussed in [2]. The boundary

conditions for Eqs. (2.1) and (2.2) take into account the injection of electrons from the electrodes under the influence of ion–electron emission [3]:

$$\frac{N_e V_t}{4} - \mu_e E N_e - \frac{\partial D_e N_e}{\partial x} = \gamma N_p V_p,$$

$$\frac{N_e V_t U_e}{4} - \mu_u E N_e U_e - \frac{\partial D_u N_e U_e}{\partial x} = \gamma N_p V_p U_e,$$

where V_t is the electron thermal velocity, and γ is the ion–electron emission coefficient.

A distinctive feature of the proposed model is the fact that it treats two groups of electrons. A justifiable objection to the conventional hydrodynamic model is that it does not correctly account for the contribution of high-energy γ-electrons to inelastic scattering processes in the plasma. Indeed, electrons emitted from the electrode surfaces pass through the layer virtually without collision and can thus build up an energy of the order of the constant plasma potential (which amounts to several dozen or even hundreds of electron-volts). A γ-electron of such high energy is capable of instigating several ionization events in the plasma. However, the hydrodynamic model deprives it of this possibility by averaging the energy U_e in Eq. (2.2) over all plasma electrons, many of which have energies of the order of the electron temperature, which is far below the plasma potential (in our case $T_e \sim$ 1-3 eV).

To circumvent this inconsistency, our model isolates γ-electrons in a special group, for which Eqs. (2.1) and (2.2) are solved separately. Electrons generated in ionization involving γ-electrons have a low energy and therefore belong to the second (low-temperature) group of electrons.

To include heating of the gas, we solve the heat-conduction equation at constant pressure

$$\frac{d\lambda\,(dT/dx)}{dx} = Q, \quad p = NT = \text{const}.$$

Here λ is the thermal conductivity, Q is the Joule heat of the gas due to energy losses by ions and electrons, and T and N are the temperature and density of the gas. The numerical algorithm used to solve the system of equations is described in [3], in which the validity of the above-described model for modeling a low-pressure (p = 13.3-133.3 Pa) rf discharge in electronegative gases is also discussed.

3. KINETIC COEFFICIENTS

Transport Cross Section. The transport cross section from [13] is used in the calculations. Measurements of the electron elastic scattering cross sections are also reported in [14-17]. Each cross section has a minimum at energies around 0.5 eV and a maximum at 2-5 eV. If we throw out the excursion cross section in [17], the other three agree to within 50%.

Cross Section for the Excitation of Vibrational Degrees of Freedom. In determining the electron distribution function, the losses of electron energy in vibrational excitation are calculated from the cross sections in [16]. The energy losses in the excitation of two levels with energy thresholds ε = 0.113 eV and 0.271 eV are taken into account. All the authors [13-16] agree on the first maximum of the cross section. The second maximum is placed at ε = 2.5 eV in [13] and at ε = 7-8 eV in [14-16]. Calculations with the vibrational cross sections from [13] yield excellent agreement with the experimentally measured drift velocity.

Adhesion Cross Section. The dissociative adhesion cross section is taken from [14] in our calculations. The electron adhesion cross section given in [17] is in good agreement with the cross section chosen for the calculations. The main dissociative adhesion channel is

$$SiH_4 + e = SiH_3^- + H.$$

Dissociation Cross Section. The total cross section for the dissociation of silane by high-energy electrons is taken from [16]. According to [4, 8], the silane molecule decomposes 75% with the formation of SiH_2 (by the schemes $SiH_4 + e = SiH_2 + H_2$ and $SiH_4 + e = SiH_2 + 2H$) and 25% with the formation of SiH_3 (by the scheme $SiH_4 + e = SiH_3 + H$). The threshold energy of the process is ε = 8.4 eV.

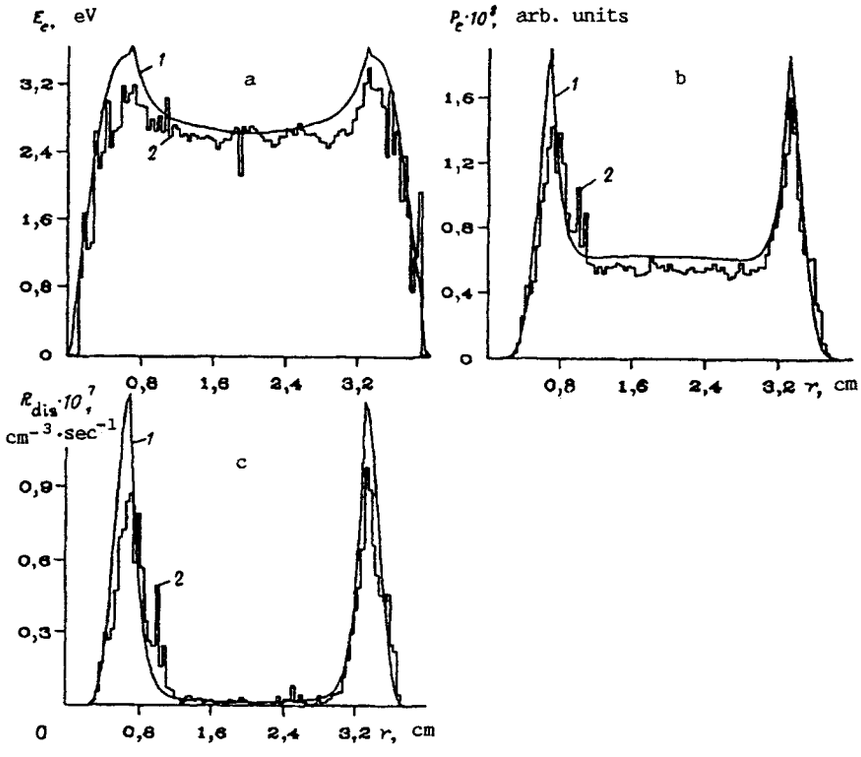

Fig. 1

Ionization Cross Section. The total ionization cross section is taken from [13] and is in good agreement with the value given in [18]. According to [19], dissociative ionization is predominant in silane, and SiH_4^+ ions are virtually nonexistent. The threshold energy of the process is $\varepsilon = 11.6$ eV.

Cross Section for the Excitation of Rotational Degrees of Freedom. The SiH_4 molecule has neither a dipole nor a quadrupole moment, hence the energy losses in rotational excitation are small [17].

4. RESULTS OF THE CALCULATIONS

In choosing the parameters for the calculations, we are guided by the experimental work of Braglia et al. [18], who used a reactor with two plane-parallel 25 × 25-cm electrodes separated by a distance D = 1-10 cm. Deposition was implemented from pure monosilane with a volumetric flow rate Q = 200 cm^3/min at atmospheric pressure for a chamber pressure p = 0.2-0.5 Pa, discharge power W = 5-80 W, and substrate temperature T_w = 20-230°C. Comparative Monte Carlo calculations of the electron kinetics are performed to justify the hydrodynamic approximation. We investigate the motion of electrons in a nonuniform, periodic field approximately characterizing the field distribution in the rf discharge:

$$E(x, t) = E_s \sin(wt) + E_k(t)\left(1 - \frac{x}{D_k(t)}\right), \quad 0 < x < D_k,$$

$$E(x, t) = E_s \sin(wt), \quad D_k < x < D - D_a,$$

$$E(x, t) = E_s \sin(wt) - E_a(t)\left(\frac{x - D}{D_a(t)} - 1\right), \quad D - D_a < x < D.$$

Here $E_k(t) = 4\pi e N_i D_k$ and $E_a(t) = 4\pi e N_i D_a$ are the fields at the electrodes, $D_k(t)$ and $D_a(t) = D_{min} + 0.5(D_{max} - D_{min})[1 \pm \cos(wt)]$ are the thicknesses of the electrode sheaths, N_i is the density of ions in the sheaths, and E_s is the field in the plasma.

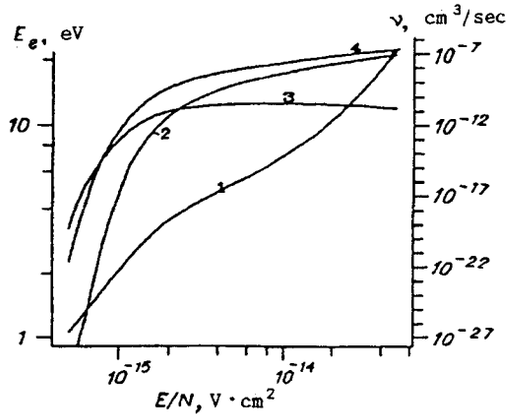

Fig. 2

TABLE 1

w = 0,05 W/cm^2, D = 4 cm					
p, Pa	w_e, %	w_i, %	ν, sec^{-1}	ε_i, eV	j_i, A/cm^2
26,7	90	10	0,68	18,5	$3\cdot10^{-5}$
40	95,5	4,5	0,43	9,8	$1,9\cdot10^{-5}$
53,3	97,3	2,7	0,3	6,5	$1,4\cdot10^{-5}$
66,7	98,2	1,8	0,23	4,6	$1,1\cdot10^{-5}$

TABLE 2

p = 66,7 Pa, D = 1.5 cm					
w, W/cm^2	w_e, %	w_i, %	ν, sec^{-1}	ε_i, eV	j_i, A/cm^2
0,05	88,3	11,7	0,69	9,3	$3,7\cdot10^{-5}$
0,07	85	15	0,94	11,6	$5,4\cdot10^{-5}$
0,09	80,7	19,3	1,2	14,2	$7,5\cdot10^{-5}$
0,128	73,8	26,2	1,75	18,8	$1,1\cdot10^{-4}$
0,2	64,4	35,6	2,7	25,6	$1,8\cdot10^{-4}$

If the values of the density N_i, the average potential U of the plasma relative to the electrode, and the electron temperature T_e in the quasineutral plasma are given, the sheath parameters D_{min} and D_{max} are determined from the condition that the total ion and electron currents onto the electrode are identical. The field in the column is usually determined by the balance between electron creation and annihilation processes. The electron kinetic equation is solved by the Monte Carlo method. The electrons are assumed to be uniformly distributed in the space between the sheaths at the initial time.

Formal restrictions are imposed on the hydrodynamic approximation at low pressures. Figure 1 shows three important discharge characteristics: the distributions of the electron energy E_e in the discharge gap (a), the power input per electron P_e (b), and the rates of dissociation R_{dis} (c), calculated in the hydrodynamic approximation and by the Monte Carlo method (curves 1 and 2, respectively) for parameters consistent with the experimental work [18] at p = 13.3 Pa, W = 0.05 W/cm^2, and D = 4 cm. The good agreement of all the curves in Fig. 1 leads to the conclusion that the hydrodynamic approximation is valid for just about all regimes in which the plasma-chemical reactor operates for the deposition of α-Si:H films.

We now analyze the results of the calculations for an rf discharge in monosilane according to the one-dimensional hydrodynamic model with two groups of electrons taken into account. As mentioned above, the constants of inelastic processes involving electrons are found by solving the kinetic equation in the binomial approximation in a uniform static electric field.

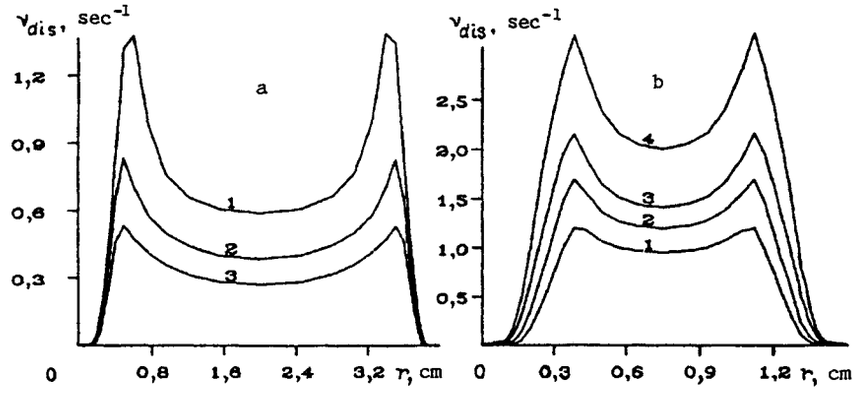

Fig. 3

Figure 2 shows the average electron energy (curve 1), the ionization frequency (curve 2), the adhesion frequency (curve 3), and the dissociation frequency (curve 4) for values of the normalized electric field E/N encompassing all operating regimes of the reactor.

To discern regular patterns of variation of the main characteristics of the rf discharge, we perform series of calculations at various values of the power input and pressure in the reactor chamber. The results are given in Tables 1 and 2, where W is the discharge power density, p is the reactor pressure, D is the interelectrode spacing, W_e and W_i are the fractions of the power input to the electronic and ionic components of the plasma, respectively, ν is the average dissociation frequency of monosilane, and ε_i and j_i are the ion energy and ion current on the electrodes.

The discharge power inputs to the ionic and electronic components of the plasma are, in the final analysis, spent in the ionization and dissociation of the gas by electrons, in the formation of ion fluxes in the electrode sheaths, and in heating of the gas. We now analyze the behavior of the period-average dissociation frequency of monosilane. Figure 3 shows the distribution of the dissociation frequency ν_{dis} in the discharge gap (total over all channels) for various pressures and power inputs. Figure 3a shows the results of the calculations for a discharge power density W = 0.05 W/cm^2, an interelectrode spacing D = 4 cm, and various chamber pressures: 1) p = 40 Pa; 2) p = 53.3 Pa; 3) p = 66.7 Pa. Figure 3b shows the results for p = 66.7 Pa, D = 1.5 cm, and various power inputs: 1) W = 0.05 W/cm^2; 2) W = 0.07 W/cm^2; 3) W = 0.09 W/cm^2; 4) W = 0.13 W/cm^2. It is evident from Fig. 3a that a reduction in the pressure at a given power density causes the dissociation frequency to increase. The reason for the this trend is that the average electron energy actually increases. On the one hand (see Table 1), the fraction of the power input to electrons decreases as the pressure is lowered (particularly when low pressures are attained) and, on the other, the electron energy is determined by the balance of their creation and annihilation or, in our situation, by the equality of the frequencies of ionization and diffusion transfer to the walls. As the pressure is lowered, the ambipolar diffusion coefficient and (to offset the increasing diffusion losses) the ionization frequency increase; this trend, in turn, indicates an increase in the electron energy. It is evident from Fig. 2 that the foregoing considerations essentially come down to the fact that we actually shift toward larger values of E/N along the horizontal axis with decreasing pressure. As the discharge power density increases, the fraction of the energy input to the electronic component of the plasma decreases; however, the electron energy increases despite this process, maintaining an essentially linear dependence of the dissociation frequency of silane, averaged over time an space in the discharge gap, on the discharge power density.

The calculations reveal the nonuniformity of the distribution of electron energy in the discharge gap (Fig. 1a), and this naturally affects the maxima at the edges of the sheaths in the frequency responses associated with inelastic collisions, such as dissociation (Fig. 3), ionization, etc. Kushner [4] attributes the high-energy tail of the electron distribution function at the boundaries between the sheaths and the plasma column to the presence of secondary electrons and the "wave riding" effect. Special calculations have brought us to the conclusion that wave riding is a purely model phenomenon associated with the solution of the nonself-consistent problem, as in electron-kinetic calculations for a model profile of the electric field by the Monte Carlo method. This phenomenon does not occur in a consistent calculation of "riding" of the electron-density and electric field profiles in the sheaths. A more plausible explanation, in our opinion, is one in which the nonuniform heating of electrons is identified with the abrupt decrease in their density at the boundaries of the sheaths, which causes the conductivity of the plasma to drop sharply in these locations and therefore intensifies the Joule heat [11].

The flux of high-energy ions onto the surface of a substrate situated on the electrode can significantly influence the film growth processes. The poor quality of amorphous silicon films grown at high discharge power densities (≥ 0.1 W/cm^2) is customarily attributed to an increase in the ratio of the volume densities of the radicals SiH_2/SiH_3 and the unfavorable surface kinetics of SiH_2 radicals from the standpoint of film quality [4, 8, 10]. Our calculations show (see Table 2) that large power densities are accompanied by substantial flows of ions with energies much greater than the binding energy of particles in the film (Si–Si $\approx$ 3 eV; Si–H $\approx$ 3 eV); such flows, of course, influence the surface kinetics, even though the mechanisms of this influence (other than the obvious possibility of etching of the film) are not altogether clear.

The reported numerical investigations of a monosilane rf-discharge plasma in the range of parameters used in the deposition of amorphous silicon films in plasma-chemical reactors lead to the following conclusions:

1. Despite its formal limitations, the hydrodynamic approximation provides a good description of processes occurring in the plasma, even at very low pressures.

2. The power input is spent mainly in heating electrons, and this accounts for the increase in the rate of dissociation of SiH_4 as the pressure is lowered at a given power density and also for the linear relation between the discharge power density and the dissociation frequency at a given pressure.

3. The nonuniformity of the distribution of electron energy in the discharge gap is dictated by the abrupt decrease in the density at the boundaries between the electrode sheaths and the plasma column.

4. Flows of high-energy ions onto the surface of the growing film occur at high rf-discharge power densities, and this can significantly influence the deposition process.

REFERENCES

1. T. Luft, "Hydrogenated amorphous silicon films," Appl. Phys. Commun., **8**, No. 1, 1 (1988).
2. V. A. Shveigert, "Numerical modeling of the stationary distribution function of electrons in a lightly ionized gas in nonuniform electric fields," Prikl. Mekh. Tekh. Fiz., No. 5, 3 (1989).
3. V. A. Shveigert, "Low-pressure rf discharge in electronegative gases," ITPM SO AN SSSR Preprint No. 8-90 [in Russian], Institute of Theoretical and Applied Mechanics, Siberian Branch of the Academy of Sciences of the USSR, Novosibirsk (1990).
4. M. J. Kushner, "On the balance between silylene and silyl radicals in rf glow discharges in silane: the effect on deposition of α-Si:H," J. Appl. Phys., **62**, 2803 (1987).
5. M. J. Kushner, "A phenomenological model for surface deposition kinetics during plasma and sputter deposition of amorphous hydrogenated silicon," J. Appl. Phys., **62**, 4763 (1987).
6. M. J. Kushner, "A model for discharge kinetics and plasma chemistry during plasma enhanced chemical vapor deposition of amorphous silicon," J. Appl. Phys., **63**, 2532 (1988).
7. M. J. Kushner, "Mechanisms for power deposition in Ar/SiH_4 capacitively coupled rf-discharges," IEEE Trans. Plasma Sci., **PS-14**, No. 2, 182 (1988).
8. A. Gallagher, "Neutral radical deposition from silane discharges," J. Appl. Phys., **63**, 2406 (1988).
9. R. C. Ross and J. Jaklic, "Plasma polymerization and deposition of amorphous hydrogenated silicon from rf and dc silane plasmas," J. Appl. Phys., **55**, 3785 (1984).
10. N. Itabashi, N. Nishiwaki, M. Magane, et al., "SiH_3 radicals density in pulsed silane plasma," Jpn. J. Appl. Phys., **29**, No. 3, 585 (1990).
11. I. D. Kaganovich and L. D. Tsendin, "Model of collisional low pressure rf-discharge," IEEE Trans. Plasma Sci., **PS-20**, No. 1, 1 (1992).
12. V. V. Boiko, Yu. A. Mankelevich, A. T. Rakhimov, et al., "Numerical investigation of an rf discharge in low-pressure, electronegative gases," Fiz. Plazmy, **15**, 218 (1989).
13. M. Kurachi and Y. Nakamura, "Electron collision cross section for monosilane molecule," J. Phys. D: Appl. Phys., **22**, 107 (1989).
14. M. Hayashi, "Effect of gas impurity for the electron drift velocities in inert gases by Boltzmann equation analysis," in: Swarm Studies and Inelastic Electron–Molecule Collisions, L. C. Pitchford et al. (eds.), Springer-Verlag, Berlin–New York (1987).

15. A. Jain and D. G. Thompson, "Elastic, inelastic, and total cross sections for x-ray and electron scattering from molecular silane," J. Phys. B: At. Mol. Phys., **20**, 2861 (1987).
16. Y. Ohmori, M. Shimozuma, and H. Tagashira, "Boltzmann equation analysis of electron swarm behaviour in monosilane," J. Phys. D: Appl. Phys., **19**, 1029 (1986).
17. K. J. Mathieson, P. G. Millican, I. S. Walker, and M. G. Curtis, "Low-energy electron collision cross sections in silane," J. Chem. Soc. Faraday Trans., **1183**, 1041 (1987).
18. G. L. Braglia, L. Romano, and M. Diligenti, "On the accuracy of experimental electron energy distributions in gases," Nuovo Cimento B, **85**, 193 (1985).
19. H. Chatham, D. Hils, R. Robertson, and A. Gallagher, "Total and partial electron collisional cross sections for CH_4, C_2H_6, SiH_4, and Si_2H_6," J. Chem. Phys., **81**, 1770 (1984).